Neural Comput & Applic (2015) 26:765–773
DOI 10.1007/s00521-014-1762-2

ORIGINAL ARTICLE

Artificial neural network method for solving the Navier–Stokes equations

M. Baymani · S. Effati · H. Niazmand · A. Kerayechian

Received: 10 October 2012 / Accepted: 16 October 2014 / Published online: 30 October 2014

Abstract In this paper, a new method based on neural network is developed for obtaining the solution of the Navier–Stokes equations in an analytical function form. The solution procedure is based upon forming a trial solution consisting of two parts. The first part directly satisfies the boundary conditions and therefore, contains no adjustable parameters. The second part is constructed such that the governing equation is satisfied inside the solution domain, while the boundary conditions remain untouched. This part involves a feed-forward neural network, containing adjustable parameters (the weights), which must be determined such that the resulting approximate error function is minimized. The details of the method are discussed, and the capabilities of the method are illustrated by solving Navier–Stokes problem with different boundary conditions. The performance of the method and the accuracy of the results are evaluated by comparing with the available numerical and analytical solutions.

M. Baymani
Department of Mathematics, Quchan University of Advanced Technology, Quchan, Iran
e-mail: m_baymani@qiet.ac.ir

S. Effati · A. Kerayechian
Department of Mathematics, Ferdowsi University of Mashhad, Mashhad, Iran

S. Effati (✉)
The Center of Excellence on Soft Computing and Intelligent Information Processing (SCIP), Ferdowsi University of Mashhad, Mashhad, Iran
e-mail: s-effati@um.ac.ir

H. Niazmand
Mechanical Engineering Department, Faculty of Engineering, Ferdowsi University of Mashhad, Mashhad, Iran

Keywords Numerical solutions · Artificial neural network · Navier–Stokes equations

1 Introduction

Developing solutions to the Navier–Stokes equations has attracted many researchers because of its practical importance in the field of fluid mechanics. However, due to the nonlinear nature of Navier–Stokes equations the main stream of the solution procedures are in fact numerical methods, which have been developed considerably in recent years because of the amazing advances in the computing power and speed. However, very limited information is available in the form of analytical functions as the Navier–Stokes solutions, especially when the nonlinear terms remain in the governing equations.

Odibat et al. [9] derived analytical solutions for the time-fractional Navier–Stokes equations in a circular tube with the help of Laplace and finite Hankel transforms. Detailed expressions for the solutions are constructed in the form of a convergent series. Muhyuddin et al. [8] presented analytical solutions of two-dimensional Navier–Stokes equations governing the unsteady incompressible flows. The solutions have been obtained using hodograph–Legendre transform method. Zhang et al. [10] used the Fourier series approach to obtain analytical solution of electroosmotic flows (EOF) in microchannels with heterogeneous zeta potentials. The mixing effects of the flow are analyzed by solving the Stokes equation with heterogeneous slip velocity boundary conditions. The obtained analytical results are compared with the numerical simulations of the Navier–Stokes equations. Horiuchi et al. [6] presented an analytical solution to the two-dimensional fluid flow in a rectangular microchannel in the vicinity of a

step change in the wall zeta potential. The stream function is determined from creeping flow approximation to the Navier–Stokes equations assuming a fixed volumetric axial flow, a constant electric field, and thin symmetric double layers. The resulting biharmonic equation is solved using a double-sided Laplace transformation, which is then inverted by Heaviside expansion. Erdoğan et al. [4] obtained an exact solution of the Navier–Stokes equation for unsteady flow over a moving plate between two sidewalls. That solution solves the problem that arising calculating shear stress at the bottom wall when the expression of velocity presented in literature is used. Dongyang et al. [2] proposed a new stable nonconforming mixed finite element scheme with second-order accuracy for the stationary Stokes and Navier–Stokes equations, in which a new nonconforming rectangular element is taken for approximating space the velocity and the bilinear element for the pressure. The optimal error estimates for the approximation of both the velocity and the pressure in L_2-norm are established, as well as one in a broken H_1-norm for the velocity.

Unfortunately, only a few analytical works are currently present in literature. One of them is the transformation of the Navier–Stokes equations to Schrodinger equation by application of Riccati equation. It has good prospects since Schrodinger equation is linear and has well-defined solutions. The method of Lie group theory is also applied in order to transform the original partial differential equations into ordinary differential systems [1]. It is concluded that an approximate series solution is obtained.

In the present study, the analytical functions as an approximate solution of the Navier–Stokes equations are developed by the use of artificial neural network (ANN). ANN has been widely used in solving partial differential equations; however, in the article, the method is extended to obtain the solution of Navier–Stokes problem. The neural network method involves approximating the solution with a function that depends, directly, on neural network. An appropriate error function is then formulated in terms of the trial solution. The resulting error function, therefore, depends on the network parameters. Thus, to obtain the required approximate solution, the error function is minimized with respect to these parameters. This procedure highlights the general features of a typical ANN numerical method. Neural network methods differ mainly by the technique of constructing trial solutions to the given problems and the way the trial solutions relate to the chosen network. The effectiveness of the method relies essentially on these techniques.

As mentioned earlier, the ANN's method has been used for solving partial differential equations by many researchers; for example, Largris et al. [7] employed ANN for solving ordinary and partial differential equations for both boundary value and initial value problems. They used multilayer perceptions to estimate the solution of differential equation. Their neural network model was trained in an interval, so the inputs of neural network model were the training points. Hayati and Karami [5] used a modified neural network to solve the Berger's equation in one-dimensional quasi-linear partial differential equation. Effati and Pakdaman [3] presented a novel method for solving fuzzy differential equations with initial conditions based on the use of feed-forward neural networks.

2 Mathematical model

Two-dimensional Navier–Stokes equations including continuity and momentum equations are considered for an incompressible laminar flow in the non-dimensional form as:

$$\begin{aligned}
&\frac{1}{Re}\Delta u - \frac{\partial p}{\partial x} = u\frac{\partial u}{\partial x} + v\frac{\partial u}{\partial y} + f_1, \quad \text{in} \quad \Omega \\
&\frac{1}{Re}\Delta v - \frac{\partial p}{\partial y} = u\frac{\partial v}{\partial x} + v\frac{\partial v}{\partial y} + f_2, \quad \text{in} \quad \Omega \\
&\frac{\partial u}{\partial x} + \frac{\partial v}{\partial y} = 0, \quad \text{in} \quad \Omega
\end{aligned} \tag{1}$$

where $\Omega \subset R^2$ is a rectangular $u(x, y)$ and $v(x, y)$ are the stream wise and normal component of the velocity field, respectively, f_1 and f_2 are the components of a given, externally applied force (e.g., gravity).

For a two-dimensional flow, a stream function $\psi(x, y)$ can be introduced as:

$$u = \frac{\partial \psi(x, y)}{\partial y}, \quad v = -\frac{\partial \psi(x, y)}{\partial x} \tag{2}$$

which satisfies the continuity equation directly. Eliminating pressure from momentum equations using stream function leads to the vorticity transport equation as follows:

$$\frac{1}{Re}\Delta^2\psi - \frac{\partial \psi}{\partial y}\Delta\left(\frac{\partial \psi}{\partial x}\right) + \frac{\partial \psi}{\partial x}\Delta\left(\frac{\partial \psi}{\partial y}\right) = \frac{\partial f_1}{\partial y} - \frac{\partial f_2}{\partial x} \tag{3}$$

Equation (3) has a unique solution if there are two boundary conditions on $\partial\Omega$.

We consider the following two boundary conditions on $\partial\Omega$ for $\psi(x, y)$:

$$\psi(x, y) = g(x, y), \tag{4}$$

$$\frac{\partial \psi}{\partial n}(x, y) = h(x, y) \tag{5}$$

where n is a unit vector normal to the $\partial\Omega$, $g(x, y)$ and $h(x, y)$ are known functions.

We present the neural network method for solving Eq. (3) with the boundary conditions (4) in the next section.

3 Description of the method

In this section, we employ a layered network to obtain an approximation solution to Navier–Stokes problem. A layered network is constructed by arranging all the neurons performing the same function in layers. These networks are further classified according to their input–output processing is progressive mechanisms. A feed-forward network is one in which processing is progressive, one-directional only. That is the output of neurons in a given layer serves as input only neurons in the proceeding layer. This type of network consists of an input layer, an output layer, and one or more hidden layers, with no interconnections among neurons in the same layer.

A feed-forward ANN is popular in the field of function approximation. In function approximation, it is customary to use linear transfer function in the input and output layers. The hidden layer(s), on the other hand, require(s) nonlinear transfer function to alter the representation of the inputs. The output of a two-layer network, $N(\vec{r},\vec{p})$, for a given input vector, $\vec{r}=(r_1,r_2,\ldots,r_n)$, is described by the weighted sum.

$$N(\vec{r},\vec{u},\vec{v},w)=\sum_{i=1}^{m} v_i f(z_i), \tag{6}$$

where f is the transfer function of hidden layer and $z_i=\sum_{j=1}^{n} w_{ij}r_j+u_i$ is the transformation variable. The output of the three-layer network, illustrated in Fig. 1, is given by.

$$N(\vec{r},\vec{u},\vec{v},\vec{w})=\sum_{i=1}^{m_1} v_i f_2\left(\sum_{j=1}^{m_2} w_{ij}^{(2)} f_1(z_j)-u_i\right), \tag{7}$$

with $z_j=\sum_{k=1}^{n} w_{jk}^{(1)} r_k+u_j$, and $\hat{w}$ is a matrix. For every additional hidden layer, the corresponding output of the network is obtained by replacing z with $f(z)$ in Eq. (6).

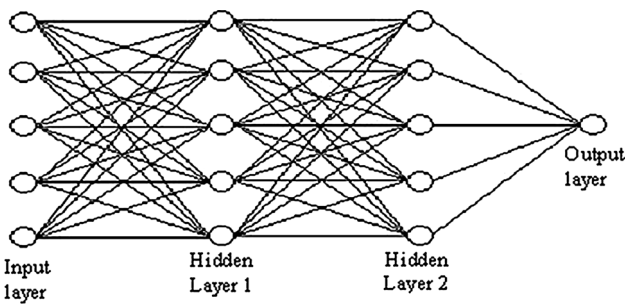

Fig. 1 A typical architecture of a multilayer feed-forward artificial neural network with two hidden layers

The output of network in the form of (6) is called parametric form. The nonparametric form of the output is:

$$N(\vec{r},\vec{v})=\sum_{i=1}^{n} v_i f_i(\vec{r}). \tag{8}$$

We denote $\overline{\Omega}=\Omega\cup\partial\Omega$. It is assumed that $f_1,f_2\in C(\overline{\Omega})$ and the solution $\psi(x,y)$ belong to $C^k(\overline{\Omega})$, the space of continuous functions with continuous partial derivatives up to k order. The set of the admissible functions

$$S=\left\{\psi\in C^k(\overline{\Omega}),\quad \Omega\subset R^2,\quad \psi=g\ \text{on}\ \partial\Omega\right\}$$

forms a linear space. It is further assumed that the domain under consideration Ω is bounded, and its boundary ∂D is sufficiently smooth (Lipschitzian).

According to the output of a three-layer network, we construct the set of function S, by defining the following trial function $\psi^{(t)}$:

$$\psi^{(t)}(r,W)=A(r)+F(r,N(r,W))$$

where $N(r,W)$ is a signal-output feed-forward neural network with parameters W and two input units fed with the input vector r. The first part of the trial solution, $A(r)$, contains no adjustable parameters, and it is designed just to satisfy the boundary conditions, while the second part, F, is constructed with no contributions to the boundary condition.

A systematic method for constructing the functional forms of both A and F for $D=[0\,L]\times[0\,h]$ is outlined in the following:

Let $\psi(0,y)=f_0(y),\ \psi(L,y)=f_1(y),\ \psi(x,0)=g_0(x)$ and $\psi(x,h)=g_1(x)$. The trial solution is written as:

$$\psi^{(t)}(x,y,W)=A(x,y)+xy(x-L)(y-h)N(x,y,W) \tag{9}$$

where $A(x,y)$ is chosen so as to satisfy the boundary conditions (BC's), namely:

$$\begin{aligned}A(x,y)=&\frac{1}{L}[(L-x)f_0(y)+xf_1(y)]\\&+\frac{(h-y)}{h}\left\{g_0(x)-\frac{1}{L}[(L-x)g_0(0)+xg_0(L)]\right\}\\&+\frac{y}{h}\left\{g_1(x)-\frac{1}{L}[(L-x)g_1(0)+xg_1(L)]\right\}\end{aligned} \tag{10}$$

To obtain a solution to the Eq. (3) with the boundary conditions (4) and (5), the collocation method is adopted, which assumes a discretization of the domain Ω and its boundary ∂D into a set points $\hat{\Omega}$ and $\hat{\partial\Omega}$.

If $\psi^{(t)}(r,W)$ denotes a trial solution with adjustable parameters W, the problem is transformed into:

$$\underset{W}{Min} \sum_{(x_i,y_i)\in \hat{D}\cup\hat{\partial D}} \left\{ \begin{array}{l} \left[\frac{1}{Re}\Delta^2\psi^{(t)} - \frac{\partial\psi^{(t)}}{\partial y}\Delta\left(\frac{\partial\psi^{(t)}}{\partial x}\right) + \frac{\partial\psi^{(t)}}{\partial x}\Delta\left(\frac{\partial\psi^{(t)}}{\partial y}\right) - \frac{\partial f_1}{\partial y} - \left(\frac{\partial f_2}{\partial x}\right)\right]^2_{(x_i,y_i)} \\ + \left(\frac{\partial\psi^{(t)}}{\partial n}(x_i,y_i) - h(x_i,y_i)\right)^2 \end{array} \right\} \tag{11}$$

Consider a multilayer with two input units, one hidden layer with M transfer function units and a linear output unit. For a given input vector $r = (x, y)$, the output of network is $N(x, y, W) = \sum_{i=1}^{M} v_i\sigma(z_i)$ where $z_i = w_i^{(x)}x + w_i^{(y)}y + b_i$, $w_i^{(x)}$ and $w_i^{(y)}$ denotes the weights from the input units x and y to the hidden unit i, v_i is the weight from the hidden unit i to the output, v_i is the bias of hidden unit i, and $\sigma(z)$ is the transfer function. The most frequently used functions for this purpose are the step function, the piecewise-linear function, hyperbolic tangent function, and the sigmoid function. However, in this work, we choose the transfer function according to the data of problem.

4 Numerical results

Let us now evaluate the capabilities of the present method by considering some examples of practical cases. For this matter, we will examine an electroosmotic flow (EOF) through a two-dimensional planar microchannel with different boundary conditions that creates relatively complex mixing flow features and a Navier–Stokes problem.

Example 4.1 Consider an electroosmotic flow (EOF) through a two-dimensional planar microchannel of height $h = 2\delta$ and length L, where $L \gg \delta$ (see Ref. [10]). The geometry can be described by reference to an orthogonal coordinate system with the x-axis in the streamwise direction and y-axis in the normal direction; see Fig. 2 for a schematic diagram of the flow geometry.

Microfluidics has a broad range of applications in chemistry and biotechnology, which involves sample injection, drug delivery, solution mixing, and separations.

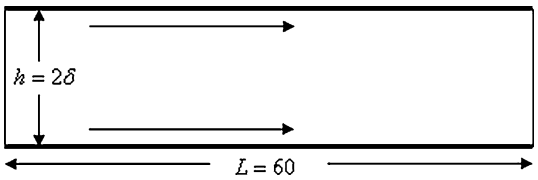

Fig. 2 A schematic diagram for a two-dimensional microchannel

All of these applications require handling fluid flow through microdevices in the low Reynolds number (Re) regime. Clearly, pressure-driven flows are not a good choice for these kinds of applications due to the enormous pressure required for liquid flow through micro-sized channels. Electroosmotic flow (EOF) is an alternative to pressure-driven flows with convenient implementation. In this section, the EOF in microchannels are examined for the purpose of rapid mixing, which involves rather complicated flow patterns. Electroosmotic flow is basically the bulk motion of liquid near a stationary surface due to an externally applied electric field. Physically, electrolytes in the vicinity of a solid surface with specified zeta potentials forms an electric double layer that can generate a flow subjected to external electric field. Mathematically, this flow can be reproduced by the application of the proper slip velocity boundary condition at the microchannel walls. In the present case, a planar microchannel with wavelike slip velocity boundary conditions is considered. Depending on the slip boundary conditions, different and interesting mixing patterns can be generated. Since microchannels are basically associated with the low Reynolds number flows, under the steady state condition, the governing equations are reduced to the Stokes equations, which in the stream function form, can be expressed as:

$$\Delta^2\psi = 0, \tag{12}$$

and the BC's are:

$$\left\{ \begin{array}{ll} \psi = Q, & \frac{\partial\psi}{\partial y} = u^t(x), \quad \text{on } y = 2 \\ \psi = 0, & \frac{\partial\psi}{\partial y} = u^b(x), \quad \text{on } y = 0 \end{array} \right. \tag{13}$$

where Q is the volume flow flux. It can be obtained from the momentum equation in the axial direction.

$$Q = \frac{\delta}{L}\int_0^L \left(u^t(x) + u^b(x)\right)dx \tag{14}$$

Zhang et al. applied the full Fourier series approach with 10 nonzero terms to analytically solve Eq. (12) with boundary conditions (13). They also performed a numerical

study by the simple finite volume technique and analyzed the resulting flow by solving the Stokes equation with different slip velocity boundary conditions. It is worth mentioning that a large number of $2{,}400 \times 80$ uniformly distributed grid points are required for their numerical scheme [10].

For comparison with the mentioned numerical and analytical solutions, an identical planar microchannel is considered with $\delta = 1$ and $L = 60$. In all cases considered here, two hidden units ($M = 2$) and $\sigma(z) = \sin(z)$ are used.

Furthermore, the solution domain is discretized into 20×8 grid points, which includes 133 interior grid points for solving the problem (11) and obtaining v_i, $w_i^{(x)}$, $w_i^{(y)}$, b_i.

We will first consider the following symmetrical slip velocity boundary condition:

$$u^t(x) = u^b(x) = 1 + 4\sin\left(\frac{2\pi x}{L}\right). \tag{15}$$

In Fig. 3, the streamlines related to the flow generated by the boundary condition (15) are presented. In this figure, the results from the ANN method (the top part) are also compared with the Zhang numerical solution (the middle) and the Fourier series solution (the bottom), where good agreements are observed.

In the next case, the slip velocities applied to the top and bottom plates are assumed to have different amplitudes,

$$\begin{cases} u^t(x) = 1 + 4\sin\left(\dfrac{2\pi x}{L}\right), \\ u^b(x) = 1 + 8\sin\left(\dfrac{2\pi x}{L}\right). \end{cases} \tag{16}$$

The resulting flow field streamlines are shown in Fig. 4. Similar to Fig. 3, the ANN results (top) are compared with the numerical results and the Fourier analytical solution (bottom). Clearly, the present method streamlines compare well with the Fourier analytical solution, while the finite volume numerical result shows some discrepancies, which indicates the present method is capable of solving the problem more accurately.

The third case is designed such that the slip velocities at the top and bottom surfaces have different phases,

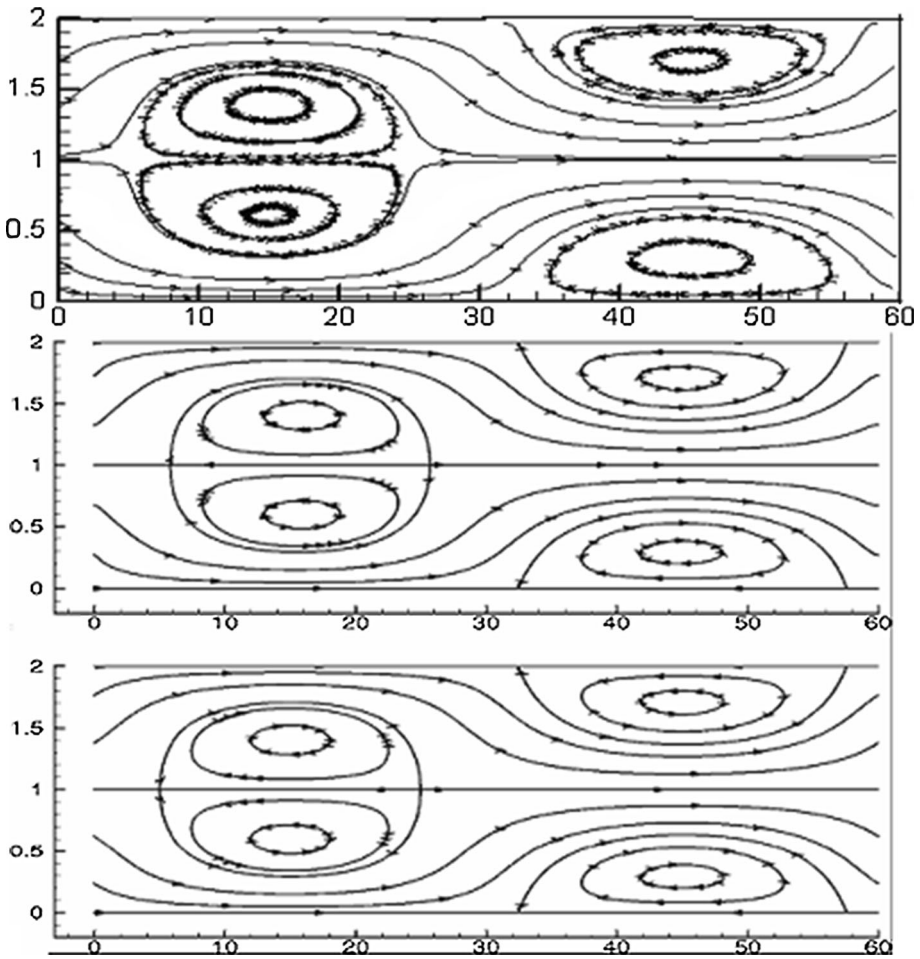

Fig. 3 Comparison of the flow field streamlines generated by symmetrical slip velocity boundary conditions: present ANN solution (*top*); numerical solution of finite volume method (*middle*) [10]; Fourier series analytical solution (*bottom*)

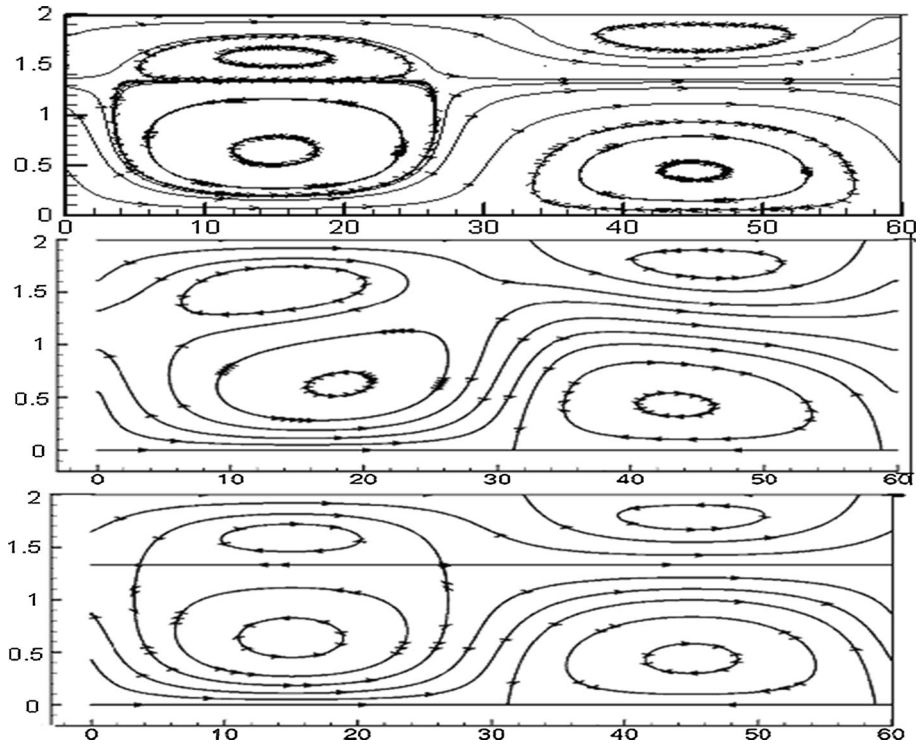

Fig. 4 Comparison of the flow field streamlines generated by asymmetrical slip velocity boundary conditions: present ANN solution (*top*); numerical solution of finite volume method (*middle*) [10]; Fourier series analytical solution (*bottom*)

$$\begin{cases} u^t(x) = 1 + 4\sin\left(\dfrac{2\pi x}{L}\right), \\ u^b(x) = 1 + 4\sin\left(\dfrac{2\pi x}{L} + \pi\right). \end{cases} \tag{17}$$

In Fig. 5, the streamlines related to this case are presented. Similar to Figs. 3 and 4, comparisons are made with the numerical results and the Fourier solution as well. For this case, all three different solution methods produce almost similar results.

As the final case, the slip velocities at the top and bottom surfaces are assumed to have different wave numbers,

$$\begin{cases} u^t(x) = 1 + 4\sin\left(\dfrac{2\pi x}{L}\right), \\ u^b(x) = 1 + 4\sin\left(\dfrac{4\pi x}{L}\right). \end{cases} \tag{18}$$

As shown in Fig. 6, the streamlines in this case exhibit rather complex patterns, including saddle points, roll, and separation point. Due to the complex nature of the mixing flow in this case, some discrepancies are observed between the present results and the Fourier solution close to the inlet and outlet of the microchannel. Clearly, the numerical solution of [10] has not been able to resolve the saddle point close to the inlet either. It is expected to improve the accuracy of the present solution if higher number of neurons are employed as shown in Fig. 7. In this figure, streamlines for flow conditions the same as those in Fig. 6 are plotted for three (top) and four (bottom) neurons. Comparing with Fig. 6, it is clear that the complex features of the flow are more accurately captured as the number of neurons are increased.

Example 4.2 The second example is devoted to the Navier–Stokes equations with the exact solution of problem (1) expressed as:

$$u^1 = 20x^2(x-1)^2y(y-1)(2y-1),$$
$$u^2 = 20y^2(y-1)^2x(x-1)(2x-1),$$
$$p = x^5 + y^5 - \frac{1}{3}$$

where f_1 and f_2 in right hand side of Eq. (1) can be generated by the above exact solutions.

Now, we solve Eq. (3) with the boundary conditions according to the above exact solutions as follows:

$$\begin{aligned} &\psi(x,y) = 0, \\ &\frac{\partial\psi}{\partial n}(x,y) = 0. \end{aligned} \tag{19}$$

Since the data (f_1 and f_2) are polynomials, we define the nonparametric trial solution $\psi^{(t)}$ as:

$$\psi^{(t)}(x,y,W) = A(x,y)\sum_{i=1}^{m}\varphi_i(x,y)$$

where $A(x,y) = (x(x-1)y(y-1))^2$ and $\varphi_i(x,y)$ are the linear independent polynomials. In this example, we

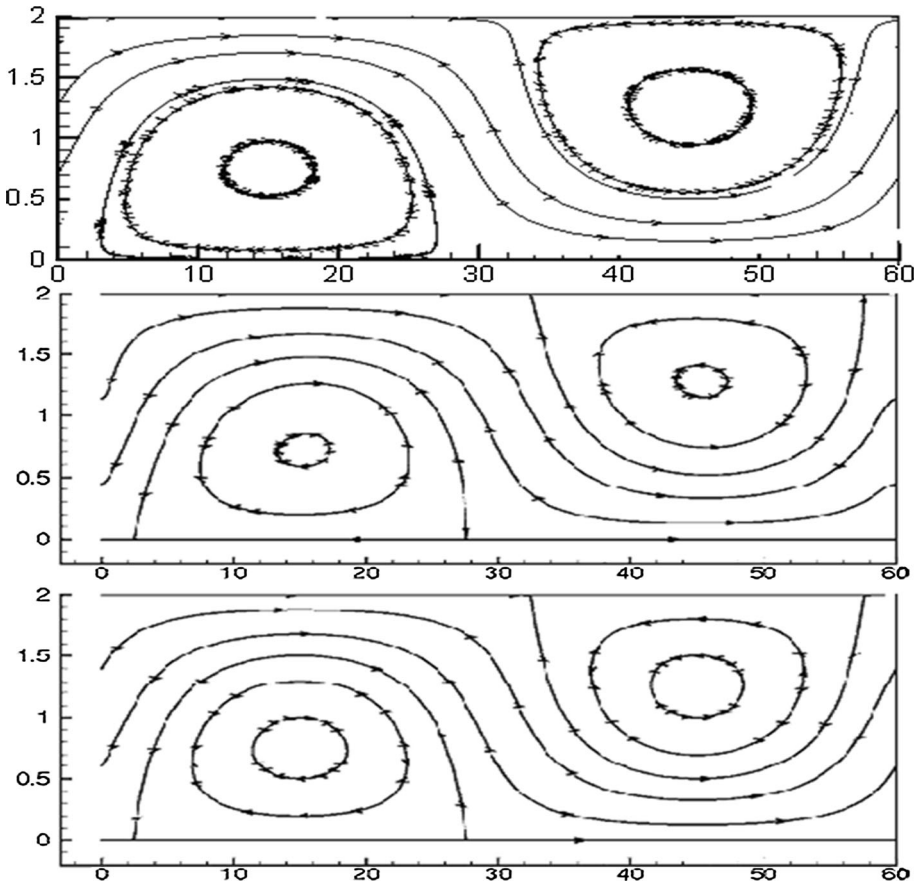

Fig. 5 Comparison of the flow field streamlines generated by asymmetrical with different phase slip velocity boundary conditions: present ANN solution (*top*); numerical solution of finite volume method (*middle*) [10]; Fourier series analytical solution (*bottom*)

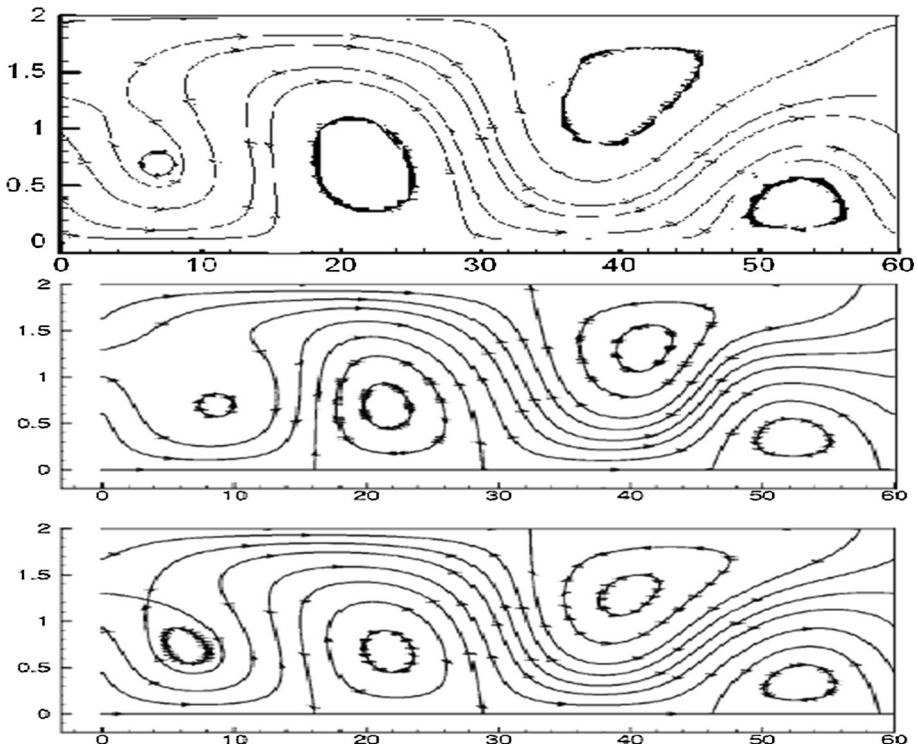

Fig. 6 Comparison of the flow field streamlines generated by asymmetrical with different wave number slip velocity boundary conditions: present ANN solution (*top*); numerical solution of finite volume method (*middle*); Fourier series analytical solution (*bottom*)

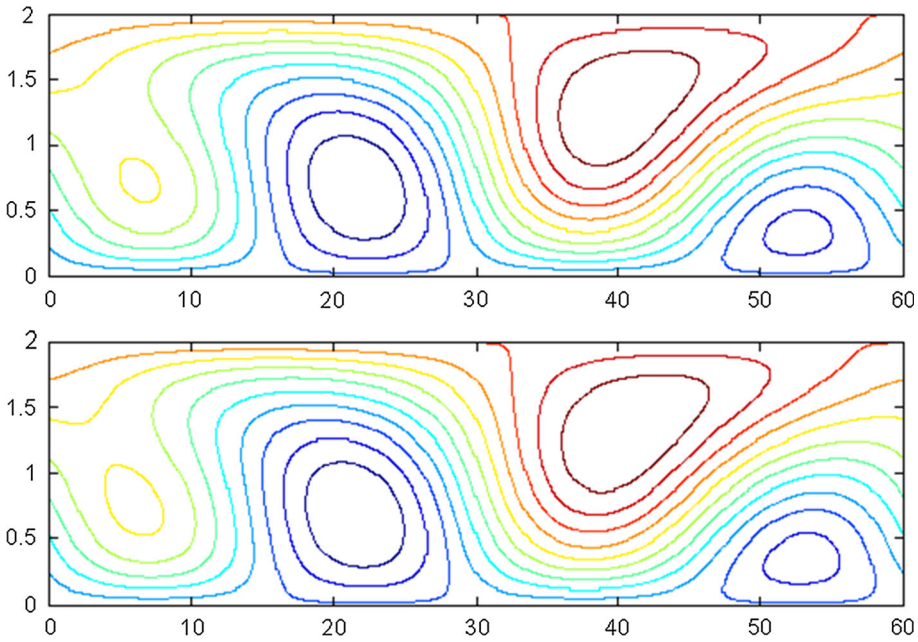

Fig. 7 Comparison of the flow field streamlines generated by asymmetrical with different wave number slip velocity boundary conditions: present ANN solution with three neurons (*top*); present ANN solution with four neurons (*bottom*)

Table 1 Error of the velocity u when $v = 0.1$ for Navier–Stokes equations

N	4^2	8^2	16^2	32^2
Finite element method				
$\|u - u_h\|_2$	8.8409e−04	3.5070e−05	1.7823e−06	1.1431e−07
$\|u - u_h\|_h$	1.0147e−01	2.0304e−02	5.0642e−03	1.3473e−03
Neural network method				
$\|u - u_h\|_2$	1.6780e−18	1.6780e−18	1.6780e−18	1.6780e−18
$\|u - u_h\|_h$	1.3046e−17	1.3046e−17	1.3046e−17	1.3046e−17

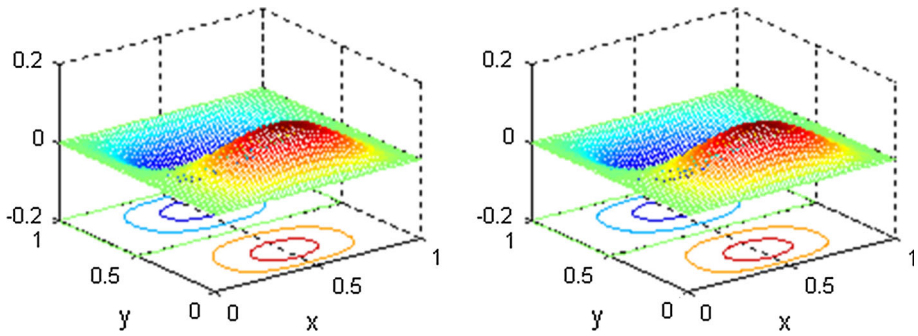

Fig. 8 The exact velocity u (*left*) and numerical velocity u_t (*right*) for Navier–Stokes equations

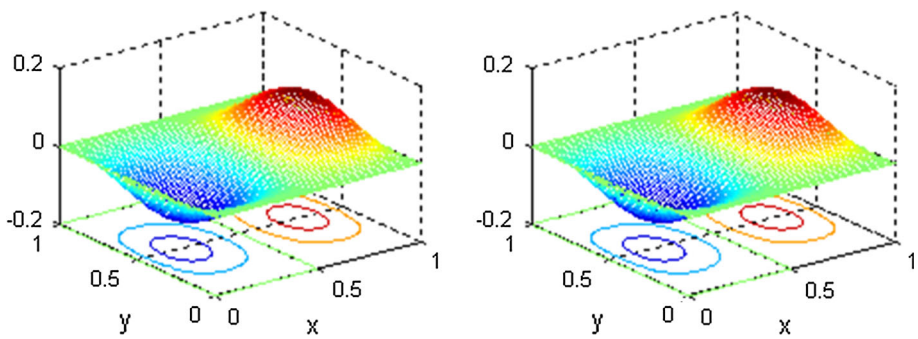

Fig. 9 The exact velocity v (*left*) and numerical velocity v_t (*right*) for Navier–Stokes equations

used the polynomial utmost of one degree and divided the space$[0,1]^2$ to 4^2. Therefore, we obtained the exact solution corresponding to the above problem. Dongyang et al. [6] solved the same problem with the finite element method by dividing the domain Ω into N uniform rectangles to obtain the errors of velocity $u = (u^1, u^2)$ under discrete energy norm and L_2 norm with $N = 4^2$; 8^2; $(1)^2$; $(32)^2$, respectively. Table 1 presents the comparison between the present neural network method and the finite element solution. Also, in Figs. 8 and 9, the numerical solutions (right) and the exact solutions (left) are depicted.

5 Conclusions

In this paper, a new method based on ANN has been developed to find approximate solution in the form of analytical function for the Navier–Stokes equations. The solution procedure and its capabilities are illustrated by solving the EOF in microchannels and the Navier–Stokes problem. The performance of the scheme and the accuracy of the results are compared with the availablenumerical and the analytical solutions in literature. The solution via ANN method is a differentiable, closed analytic form, and easily used in any subsequent calculation. The present neural network allows obtaining fast solution of the Navier–Stokes equations starting from randomly sampled data sets and refining it without wasting memory space and therefore reducing the complexity of the problem.

References

1. Christiano V, Smarandache F (2008) An exact mapping from Navier–Stokes equation to Schrodinger equation via Riccati equation. Prog Phys 1:38–39
2. Dongyang S, Jincheng R et al (2009) A new second order non-conforming mixed finite element scheme for the stationary Stokes and Navier–Stokes equations. Appl Math Comput 207:462–477
3. Effati S, pakdaman M (2010) Artificial neural network approach for solving fuzzy differential equations. Inf Sci 180:1434–1457
4. Erdogan ME, Imrak CE (2009) An analytical solution of the Navier–Stokes equation for flow over a moving plate bounded by two side walls. J Mech Eng 55(12):749–754
5. Hayati M, Karami B (2007) Feed forward neural network for solving partial differential equations. J Appl Sci 7(19):2812–2817
6. Horiuchi K, Dutta P et al (2007) Electro osmosis with step changes in zeta potential in microchannels. AIChE J 53(10):2521–2533
7. Largris IE, Likas A et al (1998) Artificial neural networks for solving ordinary and partial differential equations. IEEE Trans Neural Netw 9(5):987–1000
8. Mohyuddin M et al (2008) Exact solutions of time-dependent Navier–Stokes equations by hodograph–Legendre transformation method. Tamsui Oxf J Math Sci 24(3):257–268
9. Odibat Z, Momani S (2006) Analytical spherically symmetric solution for the time-fractional Navier–Stokes equation. Adv Theor Appl Math 1(2):97–107
10. Zhang J, Liu F et al (2006) Electro-osmotic flow and mixing in heterogeneous microchannels. Phys Rev E 73:056305–056312